Frequency-avoiding in arch bridges: a possible structural health monitoring approach

Rocco Alaggio[1], Daniele Zulli[1], Francesco Benedettini[1]
[1]*Dipartimento di Ingegneria delle Strutture, delle Acque e del Terreno, University of L'Aquila, Italy*
E-mail: rocco.alaggio@univaq.it, daniele.zulli@univaq.it, francesco.benedettini@univaq.it

Keywords: Arch bridges, frequency-avoiding, structural health monitoring.

SUMMARY. The frequency avoiding of natural frequency loci and the modal shapes hybridization are typical phenomena which take place, among other cases, in initially curved structures with a simmetry-defect, when a control parameter is varied. The phenomenon plays a key role in the explanation of a modal hybridization evidenced during the experimental tests on the "Valle Castellana" concrete, twin-arches, bridge (Provincia di Teramo, Italy). In the same way, due to high sensitivity of the hybrid modal shapes to the imperfections, the occurrence of those phenomena could be conveniently used in structural health monitoring programs. In this paper, a linear model of plane arch with an imperfection in a specific cross-section, is used as a tool in the interpretation of the behavior observed in the mentioned bridge.

1 INTRODUCTION

In symmetric structures, the crossover phenomenon takes place when two natural frequencies have a different rate of change with respect to a control parameter. It occurs, for instance, in the case of symmetric suspended cables when, increasing the elastic-geometric parameter λ^2, introduced by Irvine, the frequency of the anti-symmetric mode, which remains fixed, is crossed by the (increasing) frequency of the symmetric mode [1]. This phenomenon, with some modifications, has been observed also in the nonlinear field, for large amplitude of oscillations [2].

On the other hand, when in the structure, for some reasons, a breaking of symmetry occurs, the two involved loci of frequencies initially approach to each other. Then, for a specific value of the control parameter, a frequency avoiding (or veering) occurs and, after that, the frequencies drift away. In the veering transition, differently than the crossover case, the two involved modal shapes don't remain in their original classes but they mix each other, giving rise to mode hybridization. This phenomenon has been analyzed in case of suspended bridges under wind effect [3] and in case of r.c. arch bridges [4].

Even though standard damage detection techniques are usually based on change of the natural frequencies [5, 6], information obtained by the high sensitivity of the hybrid modal shapes to the symmetry-defect, in case of veering, could be conveniently used in structural health monitoring programs.

In the recent past, a structural health monitoring program of a cluster of bridges was carried out in Italy, in the ambit of an applied research program in cooperation between the Structural Department at University of L'Aquila (Italy) and the Public Territorial Authority "Provincia di Teramo". Among one-hundred of bridges under analysis, fifty of them were dynamically tested three times along the period 2002-2006 [7].

During the reported campaign, different typology of bridges were encountered and, among the others, six twin-arches bridges were tested. In two cases, an unexpected behavior was observed: in correspondence of an apparently symmetric configuration, the identification of spectral properties

revealed the presence of hybrid modes, not belonging to the expected classes of symmetric and anti-symmetric modes.

The occurrence of two "apparently strange" cases among the examined six, together with the consideration that in the recent past, before the large diffusion of p.r.c. technology, the typology of twin-arches bridges was largely used to cover medium spans, enlightens that the phenomenon could concern a large number of bridges, still operating in different countries.

In the paper, after introducing a linear model of a plane arch [8], the phenomena of crossing and avoiding of frequencies are discussed by means of several examples. In particular, a localized imperfection is introduced in the continuous model, and the effects on the loci of frequencies and on the modal shapes are analized. The results are used as helpful tips in the interpretation of the observed behavior of the "Valle Castellana" twin-arch bridge.

2 THE CONTINUOUS MODEL

A clamped-clamped symmetric arch, with an horizontal spring at the tip and a damage at a specified cross-section (symmetry breaking), is considered (see Fig. 1a). The Cosserat's rod theory is used to formulate the analytical model of the arch: rigid cross-sections linked to an axis line are considered. It's assumed that the inextensible, no-shear, rod, lays in a two dimensional configuration space $\mathcal{E}$. The regular curve $\bar{\mathbf{x}}(s)$ describes the axis line in the initial reference configuration $\bar{\mathcal{C}} \subset \mathcal{E}$, where $s \in [0, \ell]$ is the curvilinear abscissa and ℓ the total length. The unit orthogonal vectors $\{\bar{\mathbf{a}}_1(s), \bar{\mathbf{a}}_2(s)\}$ describe the attitude of the generic cross-section. It is assumed $\bar{\mathbf{a}}_1 = \bar{\mathbf{x}}'$ (where $'$ stands for differentiation with respect to s), i.e. the axis line is orthogonal to the generic cross-section. The initial curvature $\bar{\kappa}$, assumed uniform (circular arch), allows one to write: $\bar{\mathbf{a}}_1' = \bar{\kappa}\bar{\mathbf{a}}_2$ and $\bar{\mathbf{a}}_2' = -\bar{\kappa}\bar{\mathbf{a}}_1$.

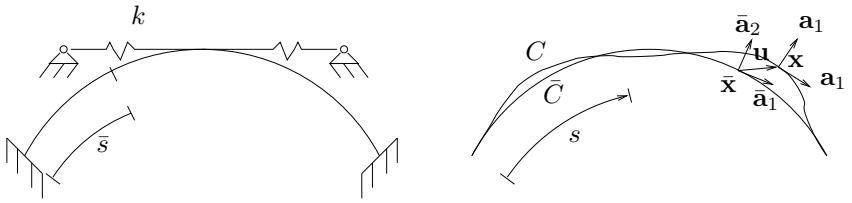

Figure 1: Model of the arch.

The deformation leads the rod from the initial configuration to the generic one $\mathcal{C}$. The axis curve in the new configuration is $\mathbf{x}(s)$ and the attitude of the cross-sections is described by two unit orthogonal vectors $\{\mathbf{a}_1(s), \mathbf{a}_2(s)\}$. The description of the deformation is obtained by the displacement vector $\mathbf{u}(s) = u(s)\bar{\mathbf{a}}_1 + v(s)\bar{\mathbf{a}}_2$ of the axis line, which carries $\bar{\mathbf{x}}(s)$ onto $\mathbf{x}(s)$, and by the the angle of rotation $\vartheta(s)$, which carries $\{\bar{\mathbf{a}}_1(s), \bar{\mathbf{a}}_2(s)\}$ onto $\{\mathbf{a}_1(s), \mathbf{a}_2(s)\}$ (see Fig. 1b). The terms u and v are the tangential and normal translation components, respectively. Therefore

$$\mathbf{x} = \bar{\mathbf{x}} + u\bar{\mathbf{a}}_1 + v\bar{\mathbf{a}}_2 \tag{1}$$

and

$$\mathbf{a}_1 = \bar{\mathbf{a}}_1 + \vartheta\bar{\mathbf{a}}_2, \quad \mathbf{a}_2 = \bar{\mathbf{a}}_2 - \vartheta\bar{\mathbf{a}}_1 \tag{2}$$

The internal constrains for inextensional, no-strain, rod are imposed, in the generic configuration, by means of the equation $\mathbf{x}' = \mathbf{a}_1$ that leads, by using the previous equations, to the following

identities:

$$u' - \bar{\kappa} v = 0, \quad v' + u\bar{\kappa} = \vartheta \tag{3}$$

The equilibrium equations are:

$$\mathbf{t}' + \mathbf{b} = \mathbf{0}, \quad \mathbf{m}' + \mathbf{x}' \times \mathbf{t} + \mathbf{c} = \mathbf{0} \tag{4}$$

where $\mathbf{t}$ and $\mathbf{m}$ are the internal force and couple, and $\mathbf{b}$ and $\mathbf{c}$ the external force and couple and $\times$ stands for the cross product. The normal and shear force components $n(s)$ and $t(s)$, so that $\mathbf{t} = n\mathbf{a}_1 + t\mathbf{a}_2$, and the bending moment $m(s)$, so that $\mathbf{m} = m(\mathbf{a}_1 \times \mathbf{a}_2)$, are introduced. Retaining only the linear part, that means considering $\kappa \simeq \bar{\kappa}$, the equilibrium equations (4) become:

$$\begin{aligned} &n' - \bar{\kappa} t + b_1 = 0 \\ &t' + \bar{\kappa} n + b_2 = 0 \\ &m' + t = 0 \end{aligned} \tag{5}$$

The response function of the material takes into account the damage in the arch localised around a section at the abscissa $\bar{s}$ (see Fig. 3a), and it is assumed in the form:

$$m(s) = EI\left[1 - \epsilon \varphi_\alpha(s - \bar{s})\right] \vartheta'(s) \tag{6}$$

where EI is the bending stiffness of the undamaged cross-section, ϵ is a nondimensional quantity representing the intensity of the damage and φ_α is a bump function defined as follows:

$$\varphi_\alpha := \begin{cases} \exp\left(1 - \frac{\alpha^2}{\alpha^2 - s^2}\right) & \text{if } |s| < \alpha \\ 0 & \text{if } |s| \geq \alpha \end{cases} \tag{7}$$

which is shown, for $\alpha = 1$, in Fig. 2. It simulates a regular contraction of the stiffness of the rod, of maximum value ϵ, in a part of the rod between the sections $\{\bar{s} - \alpha, \bar{s} + \alpha\}$.

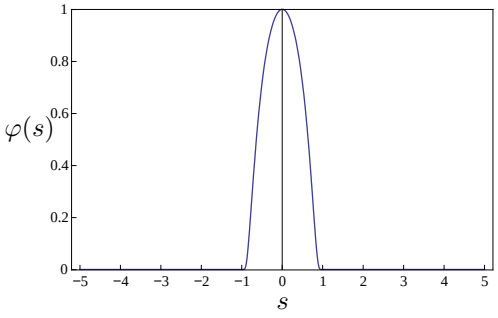

Figure 2: Bump function.

The external force components appearing in Eq. (5) contain both the continuous inertial forces and the punctual elastic force due to the spring, applied at the section at $s = \ell/2$:

$$b_1(s) = -\rho A \ddot{u}(s) - k u(s) \delta\left(s - \frac{\ell}{2}\right), \quad b_2(s) = -\rho A \ddot{v}(s) \tag{8}$$

where k is the elastic stiffness of the spring, $\delta(s-\frac{\ell}{2})$ is the Dirac function cenetred at $s=\frac{\ell}{2}$ and the dot stands for differentiation with respect to the time. Therefore, the complete system of partial differential equations describing the free dynamics of the damaged arch, with elastic spring, assumes the following form:

$$\begin{aligned}
&u' - \bar{\kappa} v = 0 \\
&v' + u\bar{\kappa} - \vartheta = 0 \\
&n' - \bar{\kappa} t - \rho A \ddot{u} - k u \delta(s-\ell/2) = 0 \\
&t' + \bar{\kappa} n - \rho A \ddot{v} = 0 \\
&m' + t = 0 \\
&EI\left[1 - \epsilon\varphi_\alpha(s-\bar{s})\right]\vartheta' - m = 0
\end{aligned} \tag{9}$$

In the case of clamped-clamped arch, the following geometric boundary conditions must be added to the system:

$$\begin{aligned}
&u(0) = 0, \qquad v(0) = 0, \qquad \vartheta(0) = 0 \\
&u(\ell) = 0, \qquad v(\ell) = 0, \qquad \vartheta(\ell) = 0
\end{aligned} \tag{10}$$

3 THE DISCRETE MODEL

A Galerkin procedure is applied to the system (9), using as shape functions the first four eigenvectors of the perfect arch without spring ($\epsilon = 0$, $k = 0$). If $\mathbf{\Phi}(s)$ is the state vector of the system (9), i.e.

$$\mathbf{\Phi}(s) = \{u, v, \vartheta, n, t, m\}^T \tag{11}$$

and $\tilde{\mathbf{\Phi}}_j(s)$ is the j-th eigenvector obtained for $\epsilon = k = 0$, the projection is done by posing $\mathbf{\Phi}(s) = \sum_{j=1}^{4} q_j(t)\tilde{\mathbf{\Phi}}_j(s)$, with $q_j(t)$ time-dependent unknown modal amplitudes. A discrete system of the following type is obtained:

$$\ddot{\mathbf{q}} + (\mathbf{K} + k\mathbf{G} + \epsilon\mathbf{H})\mathbf{q} = \mathbf{0} \tag{12}$$

where $\mathbf{q} = \{q_1, q_2, q_3, q_4\}^T$, and

$$\mathbf{K} = \begin{bmatrix} \tilde{\omega}_1^2 & 0 & 0 & 0 \\ 0 & \tilde{\omega}_2^2 & 0 & 0 \\ 0 & 0 & \tilde{\omega}_3^2 & 0 \\ 0 & 0 & 0 & \tilde{\omega}_4^2 \end{bmatrix}, \ \mathbf{G} = \begin{bmatrix} g_{11} & 0 & g_{13} & 0 \\ 0 & 0 & 0 & 0 \\ g_{13} & 0 & g_{33} & 0 \\ 0 & 0 & 0 & 0 \end{bmatrix}, \ \mathbf{H} = \begin{bmatrix} h_{11} & h_{12} & h_{13} & h_{14} \\ h_{12} & h_{22} & h_{23} & h_{24} \\ h_{13} & h_{23} & h_{33} & h_{34} \\ h_{14} & h_{24} & h_{34} & h_{44} \end{bmatrix} \tag{13}$$

are the perfect stiffness matrix ($\mathbf{K}$) and the stiffness correction matrices due to the spring ($\mathbf{G}$) and to the damage effects ($\mathbf{H}$), respectively. The matrix $\mathbf{G}$ contains just four terms different from zero, the only ones corresponding to anti-symmetric modes (mode 1 and 3). The expressions of the coefficients are reported in Appendix A.

The free dynamics of the system (12) is analyzed. It admits non-trivial solutions of type $\mathbf{q} = \mathbf{c}e^{i\omega t}$, where $\mathbf{c}$ and ω are unknown and i is the imaginary unit. This solution, substituted in Eq. (12), produces the following algebraic eigenvalue problem:

$$\mathbf{A}(\omega)\mathbf{c} = \mathbf{0} \tag{14}$$

where $\mathbf{A}(\omega) = -\omega^2\mathbf{I} + \mathbf{K} + k\mathbf{G} + \epsilon\mathbf{H}$, being $\mathbf{I}$ the identity matrix of order four. Equation (14) admits non-trivial solution if and only if $\det \mathbf{A} = 0$. This characteristic equation allows one to evaluate the

natural frequencies ω_j of the system. In corrispondence of each frequencies, it is possible to solve the system (14), to obtain the eigenvectors $\mathbf{c}_j$, and to reconstruct the contiunous, approximate, modes of the system (12) as

$$\mathbf{\Phi}_i(s) = \sum_{i=1}^{4} c_{ji} \tilde{\mathbf{\Phi}}_i(s) \tag{15}$$

being c_{ji} the i-th component of the vector $\mathbf{c}_j$.

4 SOLUTION

When both the spring and the damage are absent ($k = \epsilon = 0$), the natural frequencies of the system (12) come down to those of the perfect system: $\omega_j \equiv \tilde{\omega}_j$, $j = 1, \ldots, 4$. In this case, the eigenvectors $\mathbf{c}_j$ coincide to the vectors of the natural base ($\mathbf{c}_j \equiv \mathbf{e}_j$), since the system (12) is uncoupled. It means that the eigenfunctions of the arch are exactly those used as shape functions in the Galerkin projection. For specific numerical values of the parameters of the arch (bendig stiffness $EI = 2.025 \times 10^7$ Nm^2, mass per unit lenght $\rho A = 225$ Kg/m, radius $R = 40$ m, length of the axis line $\ell = 20$ m) the frequencies assume the values $\omega_1 = 44.79$ rad/s, $\omega_2 = 81.16$ rad/s, $\omega_3 = 146.17$ rad/s, $\omega_4 = 212.16$ rad/s, and the corresponding eigenfunctions are reported in Fig. 3.

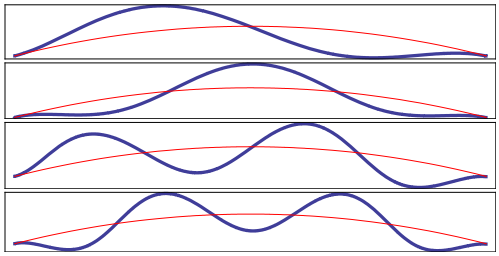

Figure 3: Eigenfunctions of the perfect arch: (a) first anti-symmetric mode; (b) first symmetric mode; (c) second anti-symmetric mode; (d) second symmetric mode. Red thin line: initial configuration; blue thick line: modal displacement.

When the spring is present in no-damage condition ($k \neq 0$, $\epsilon = 0$), the natural frequencies and shapes of the symmetric modes remain unchanged: $\omega_j = \tilde{\omega}_j$, $\mathbf{c}_j \equiv \mathbf{e}_j$, $j = 2, 4$, while the anti-symmetric modes are affected by the spring. Their frequencies vary significantly (see Fig. 5a): in corrispondence of the value $k \approx 4 \times 10^8$ N/m, a crossing between the first anti-symmetric and symmetric modes occours; they invert their order without any interactions, and some modifications of the shape of anti-symmetric mode is observed (see Fig. 4).

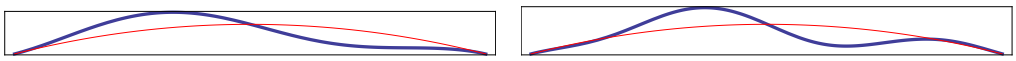

Figure 4: First anti-symmetric mode before and after the first crossover when $\epsilon = 0$: (a) $k = 1 \times 10^8$ N/m; (b) $k = 1 \times 10^9$ N/m. Red thin line: initial configuration; blue thick line: modal displacement.

In corrispondence of the value $k \approx 2 \times 10^9$ N/m a veering between the first anti-symmetric and the second anti-symmetric modes occurs and, consequently, the corresponding shapes are hybrid,

but keeping their properties of anti-symmetry (see Fig. 6). In corrispondence of the value $k \approx 4\times10^9$ N/m, a secondary crossing between the second anti-symmetric and symmetric modes occurs. Good agreement is obtained, between the analytical frequencies and those obtained by using a FE model (markers in Fig. 5a): for higher values of the parameter k, the agreement is less accurate (diamond markers in Fig. 5a), because the modal shape of the FE model starts to become hybrid near a secondary veering, which takes place out of the ranges of the diagram; to get better agreement, a further anti-symmetric mode should be added in the discretization procedure. Hence, it can be observed that, quite far in the left side of the first veering zone, that occurs at $k \approx 2 \times 10^9$ N/m, all the modes, except the first anti-symmetric one, coincide to those of the model without spring; therefore $\mathbf{c}_2 \equiv \mathbf{e}_2$ and $\mathbf{c}_1 = \alpha_1\mathbf{e}_1 + \alpha_3\mathbf{e}_3$, where α_1, α_3 are coefficients which depend on k.

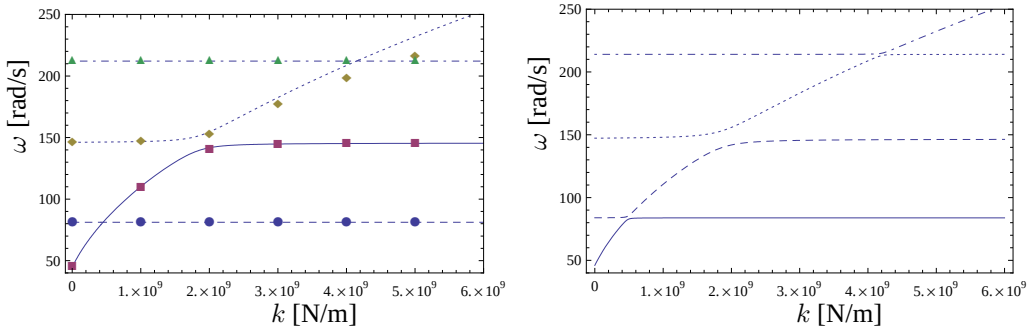

Figure 5: Modal frequencies in function of the intensity of the spring in no-damage condition (a) and in damage condition ($\epsilon = 0.3$) (b). Markers: FEM.

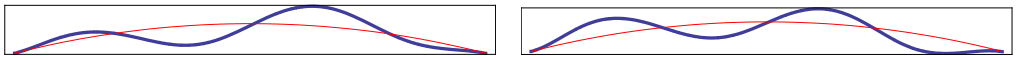

Figure 6: Hybrid eigenfunctions of the arch with the spring ($k = 2 \times 10^9$ N/m): (a) second mode; (b) third mode. Red thin line: initial configuration; blue thick line: modal displacement.

When both spring and damage are present ($k \neq 0$, $\epsilon \neq 0$, for $\bar{s} = \ell/4$), all the modal frequencies and shapes are modified. In particular, the crossing phenomena observed in the symmetric configuration, at $k \approx 2 \times 10^9$ N/m and at $k \approx 4 \times 10^9$ N/m in Fig. 5a, turn into veering (see Fig. 5b); the modal shapes, near these vaues of k, are hybrid and lose their proprerty of symmetry and anti-symmetry (see Fig. 7). The regions of values of k where the modal shapes are hybrid are as wider as the damage increases. An estimation of the wideness of the hybridization region can be obtained by evaluating the MAC index between one hybrid mode $\mathbf{\Phi}_i$, calculated for some k and ϵ, and one mode calculated for the same k, but without damage (referred as $\bar{\mathbf{\Phi}}_i$); focusing the attention to the first veering region ($k \approx 4 \times 10^8$ N/m), the modes calculated with $k \neq 0$ and $\epsilon = 0$ reduce to $\bar{\mathbf{\Phi}}_i = \tilde{\mathbf{\Phi}}_j$, $(j = 2, \ldots 4)$, while $\bar{\mathbf{\Phi}}_1 = \alpha_1\tilde{\mathbf{\Phi}}_1 + \alpha_3\tilde{\mathbf{\Phi}}_3$. Therefore the MAC index is:

$$\text{MAC}_{ij} = \frac{\left(\int_0^\ell \mathbf{\Phi}_i \cdot \bar{\mathbf{\Phi}}_j ds\right)^2}{\left(\int_0^\ell \mathbf{\Phi}_i \cdot \mathbf{\Phi}_i ds\right)\left(\int_0^\ell \bar{\mathbf{\Phi}}_j \cdot \bar{\mathbf{\Phi}}_j ds\right)} \tag{16}$$

where the dot stands for the scalar product. By using Eq. (15) and the orthogonality of the eigenvectors $\tilde{\mathbf{\Phi}}_j$, Eq. (16) becomes:

$$\mathrm{MAC}_{ij} = \frac{\left(\mathbf{c}_i \cdot \mathbf{e}_j\right)^2}{\left(\mathbf{c}_i \cdot \mathbf{c}_i\right)\left(\mathbf{e}_j \cdot \mathbf{e}_j\right)} = \frac{c_{ij}^2}{||\mathbf{c}_i||^2} \tag{17}$$

for $j = 2, 3, 4$ and, in the case $j = 1$,

$$\mathrm{MAC}_{i1} = \frac{\left(\mathbf{c}_i \cdot (\alpha_1 \mathbf{e}_1 + \alpha_3 \mathbf{e}_3)\right)^2}{\left(\mathbf{c}_i \cdot \mathbf{c}_i\right)\left((\alpha_1 \mathbf{e}_1 + \alpha_3 \mathbf{e}_3) \cdot (\alpha_1 \mathbf{e}_1 + \alpha_3 \mathbf{e}_3)\right)} = \frac{(\alpha_1 c_{i1} + \alpha_3 c_{i3})^2}{||\mathbf{c}_i||^2(\alpha_1^2 + \alpha_3^2)} \tag{18}$$

which assume values between 0 and 1.

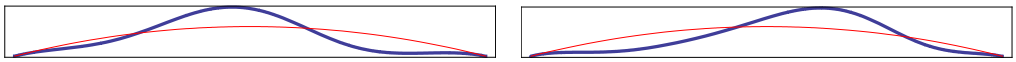

Figure 7: Eigenfunctions of the arch with the spring and damage ($k = 6 \times 10^8$ N/m, $\epsilon = 0.4$): (a) first mode; (b) second mode. Red thin line: initial configuration; blue thick line: modal displacement.

Figure 8a represents the MAC index between the first anti-symmetic mode, obtained in presence of damage and spring, and the first symmetic mode, obtained in presence of the spring without damage, in function of both the spring and damage intensities. When damage is absent (section at $\epsilon = 0$), the index is always zero. When damage is present, the MAC index assumes values different from zero around the value of $k \approx 4.5 \times 10^8$ N/m, and the region where MAC $\neq 0$, i.e. the region where the modes in presence of damage are hybrid, is as wider as damage increases. However, if the section where the damage is localized, is closer to the tip of the arch, the hybridization is extended in a smaller region (decreasing defect of symmetry).

Fig. 8b, which shows the contour plot of the MAC index in function of k and ϵ, can be used to obtain a representation of the damage evolution, observed at different times, when two hybrid modes are observed and their frequencies ω_1, ω_2 and shapes $\mathbf{\Phi}_1, \mathbf{\Phi}_2$ are identified: A given frequency separation of two subsequent modes is obtainable for different values of the "structural" parameter k and damage ϵ at different "detuning" from the nominal value of k, producing the crossover on the perfect system. Giving a frequency separation $\delta = \frac{\omega_2 - \omega_1}{\omega_1}$ between the two hybrid modes, it is possible to find two loci in the plane $\{k, \epsilon\}$ (the red thick lines in Fig. 8b) coherent with such a value. Only two couples of values $[k, \epsilon]$ are however coherent with a particular MAC (green points in Fig. 8b). They can be referred as: defect-dependent-state-points. The located points are in direct correspondance with the mechanism producing the defect of symmetry originating the hybridization, resulting very sensitive to the defect intensity. In a real case (as the one presented in the next Section), in absence of a direct measure of an occurring damage or in the case of damage not yet localized, monitoring the evolution of the defect-dependent-state-point or damage-state-point (the green point Fig. 8b) by means of a monitoring program of modal characteristics, permits to follow its evolution and to evaluate the relevant velocity. By using a validated FE model reproducing the transition, it is possible to evaluate the critical value of $[\delta, \mathrm{MAC}]$ associated to a specific limit state. In particular, the updated model allows one to locate the position of the damage-state-point and then, once the damage intensity is further increased, the state corresponding to a settled limit condition. The resulting plot represents a path of evolution of the state of the structure as the damage changes and a valid mean to control the structural condition.

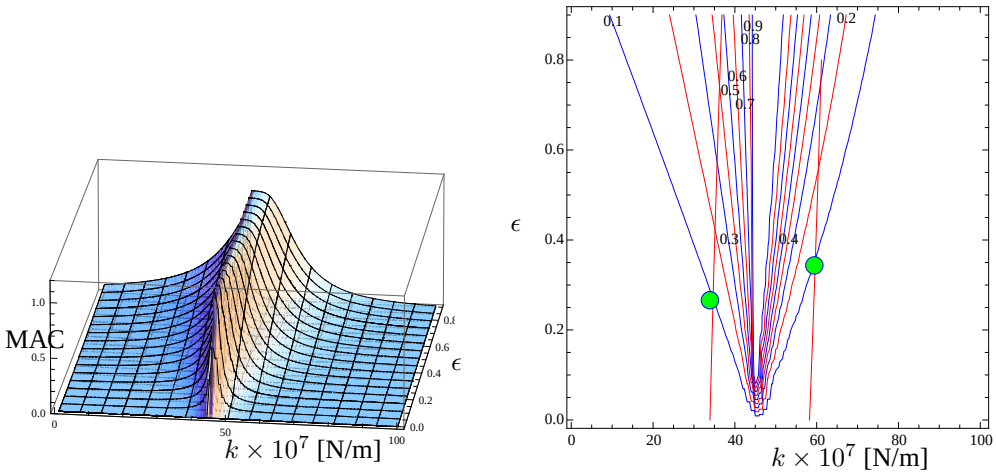

Figure 8: MAC index between the first anti-symmetric mode in presence of damage and the first simmetric mode in absence of damage, in function of k and ϵ (a); contour plot of the MAC index and loci of couples $\{k, \epsilon\}$ for fixed δ (b).

5 THE FREQUENCY AVOIDING AND MODE HYBRIDIZATION IN THE VALLE CASTELLANA ARCH BRIDGE

When a "real structure" is considered instead of a mathematical model, the variation of structural parameters is not meaningful. Notwithstanding, apparently strange behaviors, provided by the results of experimental tests, can be unfolded in the framework of the described phenomena.

During an extended campaign of repeated dynamical tests on a cluster of bridges, maintained by a Public Territorial Authority in the Abruzzo Region, in Italy, six twin-arches bridges have been analyzed. Among the six, two of them exhibited an apparently strange behavior during the tests, showing, in correspondence of a nominal symmetric geometry, two subsequent hybrid modes. In the case of the Valle Castellana bridge (Fig. 9), the first two modes having close frequencies correspond to two modes not belonging to the expected symmetric and anti-symmetric classes (Fig. 10):

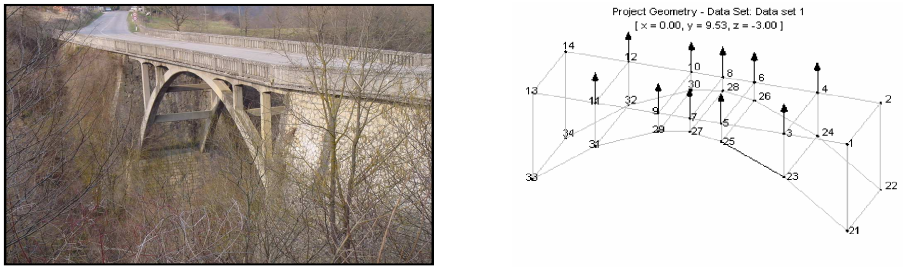

Figure 9: The twin-arch Valle Castellana bridge (a) and the accelerometers set-up (b).

The two modes in Fig. 10b clearly appear as a different combination of a symmetric mode having three half waves on the span and of an anti-symmetric mode having two half waves on the span. The

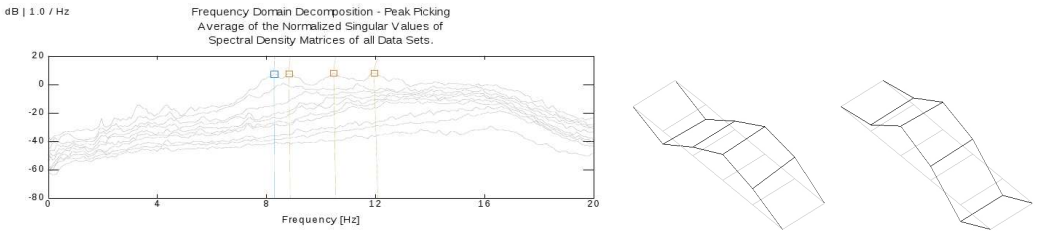

Figure 10: The singular values of the spectral density matrix (a) and the two identified hybrid modes (b).

resulting hybrid modes appear as a couple of flexural modes having respectively a bigger (smaller) half wave on the left (right) part of the deck. This kind of modal interaction could be explained by means of the theory discussed above: considering that the observed hybridization range is quite wide (hybrid modes have frequencies differing of about 9%), it was easy to forecast a lost of symmetry probably due to a localized damage. Following this idea and using a FE model of the analyzed structure, after evidencing a suitable unfolding parameter and introducing a breaking of the symmetry, it was possible to obtain a veering sequence exactly reproducing the observed hybrid modes.

In Fig. 11 the results of the eigen-analysis on the FE model of the Valle Castellana bridge are shown. It is evident that the introduced localized loss of symmetry, because of the particular tuning of elastic-geometric-inertial parameters, could be the cause of the sequence of hybrid modes identified during the tests. Due to high sensitivity of hybrid modal shapes to the imperfections, the occurrence of this phenomenon could be conveniently used to evaluate the loss of symmetry affecting the bridge in the framework of a structural health monitoring program.

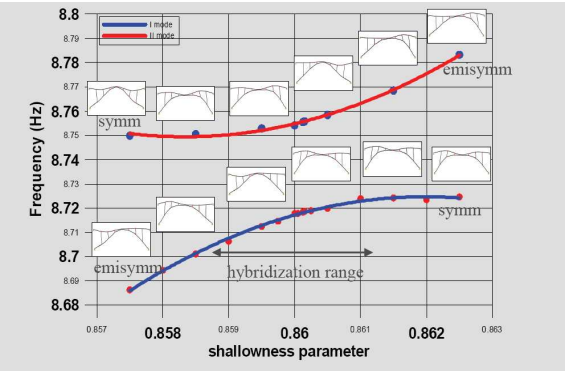

Figure 11: The veering transition in the FE model of the Valle Castellana twin-arch bridge.

6 CONCLUSIONS

This paper gives reason for the apparently strange behavior observed in the r.c. twin-arch "Valle Castellana" bridge (Provincia di Teramo, Italy), object of several dynamical tests by the Structural Department at University of L'Aquila (Italy). In particular, hybrid modes have been identified, while simple symmetric and anti-symmetric modes were expected. Therefore a linear model of plane

arch, with a loss of symmetry due to a localized damage, is introduced as a tool to describe the phenomena of crossing and veering of natural frequencies. The phenomena are described in terms of the variation of a suitable control parameter. Moreover, it is observed how the localized damage produces the hybridization of the modal shapes, which is more evident as the intensity the damage increases.

References

[1] Irvine, M., *Cable structures*, MIT Press, Cambridge, Mass, (1981).

[2] Benedettini, F., Rega, G. and Vestroni, F., "Parametric analysis of large amplitude free vibrations of a suspended cable" *Int. J. of Solids and Structures*, 20, 95-105 (1981).

[3] Chen, X. and Kareem, A., "Curve veering of eigenvalue loci of bridges with aeroelastic effects" *Engr. Mechanics*, 129(2), 146-159 (2003).

[4] Gentile, C. and Taliercio, A., "The phenomenon of veering in the assessment of r.c. arch bridges", in *Proc. 5th International Conference on Arch Bridges (Arch-07)*, Madeira, Portugal, September 12-14, 2007, 425-431 (2007).

[5] Cerri, M. N., and Vestroni, F., "Identification of damage due to open cracks by change of measured frequencies" *Proc. of XVI Conf. of Italian Association of Theoretical and Applied Mechanics, AIMETA*, Ferrara, 9-12 September 2003, CD-ROM (2003).

[6] Cerri, M. N. and Ruta, G. C., "Detection of localized damage in plane circular arch by frequency data" *J. of Sound and Vibration*, 270, 39-59 (2004).

[7] Benedettini, F., Alaggio, R. and Manetta, P., "Arch bridges in Provincia di Teramo: tests, identification and numerical models", in *Proc. 1st International Operational Modal Analysis Conference*, Copenhagen, Denmark, April 26-27, 2005, 225-236 (2005).

[8] Henrych, J., *The Dynamics of Arches and Frames*, Translated by R. Major, Amsterdam , Elsevier (1984).

A COEFFICIENTS OF THE DISCRETE SYSTEM

In this Section, the expression of the coefficients of the linear algebraic system (14) are reported. Calling $\mathbf{\Phi}_i(s) = \{u_i, v_i, \vartheta_i, n_i, t_i, m_i\}^T$ the i-th eigenvector ($i = 1, \dots 4$) and defining the modal masses $m_i := \int_0^\ell \rho A(u_i^2 + v_i^2) ds$, the coefficients of the stiffness matrices (13) read ($i, j = 1, \dots 4$):

$$
\begin{aligned}
\tilde{\omega}_i^2 &= \frac{1}{m_i} \int_0^\ell \left[(n_i' - \bar{\kappa} t_i) u_i + (t_i' + \bar{\kappa} n_i) v_i \right] ds \\
g_{ij} &= \frac{1}{m_i} \int_0^\ell u_i u_j \delta \left(s - \frac{\ell}{2} \right) ds = \frac{u_i \left(\frac{\ell}{2}\right) u_j \left(\frac{\ell}{2}\right)}{m_i} \\
h_{ij} &= \frac{1}{m_i} \int_0^\ell (\vartheta_i \vartheta_j'' \varphi_\alpha (s - \bar{s}) + \vartheta_i \vartheta_j' \varphi_\alpha' (s - \bar{s})) ds
\end{aligned}
\tag{19}
$$